HHS Public Access

Author manuscript

J Am Coll Cardiol. Author manuscript; available in PMC 2019 August 21.

Published in final edited form as:

J Am Coll Cardiol. 2018 August 21; 72(8): 885–904. doi:10.1016/j.jacc.2018.05.061.

Deficiency of GATA3-Positive Macrophages Improves Cardiac Function Following Myocardial Infarction or Pressure Overload Hypertrophy

Mingjie Yang, PHD, **Lei Song, MD**, **Lai Wang, MD**, **Ada Yukht, MS**, **Haley Ruther, MS**, **Fuqiang Li, PHD**, **Minghui Qin, PHD**, **Homayon Ghiasi, PHD**, **Behrooz G Sharifi, PHD**, and **Prediman K. Shah, MD**

Oppenheimer Atherosclerosis Research Center, Cedars Sinai Smidt Heart Institute, and Department of Surgery, Cedars-Sinai Medical Center, Los Angeles, California

Abstract

BACKGROUND: Macrophages are highly plastic cells that play an important role in the pathogenesis of cardiovascular disease.

OBJECTIVES: The authors investigated the role of GATA3-positive macrophages in modulating cardiac function after myocardial infarction (MI) or in response to pressure overload hypertrophy.

METHODS: Myeloid-specific GATA3-deficient (mGATA3KO) mice were generated; MI or pressure overload were induced, and cardiac function was determined by echocardiography. GATA3-sufficient Cre mice were used as a control. Immunohistochemical staining, flow cytometry, MILLIPLEX Mouse Cytokine/Chemokine Assay, cultured macrophages, quantitative real-time polymerase chain reaction, and western blot were used to determine the role of GATA3 in macrophages.

RESULTS: GATA3-positive macrophages rapidly accumulated in the infarcted region of the myocardium after acute MI. Deficiency of GATA3-positive macrophages led to a significant improvement of cardiac function in response to acute MI or pressure overload hypertrophy compared with the control. This improvement was associated with the presence of a large number of proinflammatory $Ly6C^{hi}$ monocytes/macrophages and fewer reparative $Ly6C^{lo}$ macrophages in

Address for Correspondence: Dr. Behrooz G. Sharifi, Oppenheimer Atherosclerosis Research Center, Division of Cardiology, Cedar-Sinai Smidt Heart Institute, Cedar-Sinai Medical Center, AHSP # 9307, 8700 Beverly Blvd., Los Angeles, California 90048, Telephone: (310) 423-7621, Fax: (310) 967-3805, Sharifi@cshs.org.

PERSPECTIVES

COMPETENCY IN MEDICAL KNOWLEDGE: Inflammation modulates LV remodeling in murine models of coronary occlusion or pressure overload. In this study, myocardial infiltration of monocytes-macrophages deficient in GATA3 was associated with less adverse LV remodeling and better preservation of LVEF, demonstrating the complex role of macrophage phenotypes in LV remodeling.

TRANSLATIONAL OUTLOOK: Further studies are needed to define the role of myeloid expression of GATA3 in LV remodeling in human subjects after acute MI or LV pressure load. If confirmed, modulating macrophage expression of GATA3 may provide a novel therapeutic target to attenuate adverse LV remodeling.

Disclosures: The authors have reported that they have no relationships relevant to the contents of this paper to disclose.

the myocardium of mGATA3KO mice compared with control mice. Analysis of serum proteins from the 2 mouse genotypes revealed no major changes in the profile of serum growth factors and cytokines between the 2 mice genotypes before and after MI. GATA3 was found to be specifically and transiently induced by interleukin 4 in cultured macrophages through activity of the proximal promoter, whereas the distal promoter remained silent. In addition, the absence of GATA3 in macrophages markedly attenuated arginase-1 expression in cultured macrophages.

CONCLUSIONS: We demonstrated that the presence of GATA3-positive macrophages adversely affects remodeling of the myocardium in response to ischemia or pressure overload, whereas the absence of these macrophages led to a significant improvement in cardiac function. Targeting of signaling pathways that lead to the expression of GATA3 in macrophages may have favorable cardiac outcomes.

CONDENSED ABSTRACT:

Monocytes/macrophages play a critical role in the pathogenesis of cardiac diseases. The authors identified a subset of macrophages, GATA3-positive, that accumulate in the myocardium after myocardial infarction (MI). Genetic depletion of this macrophage subset significantly improved cardiac function after MI or in response to pressure overload. The absence of GATA3-positive macrophages reduced the frequency of $Ly6C^{lo}$ macrophages in the ischemic myocardium. The data suggest that therapeutic targeting of GATA3 signaling in macrophages may improve the outcome of cardiac diseases.

Keywords

cardiac hypertrophy; inflammation; macrophage; transcription factor

INTRODUCTION

Macrophages are important effectors of innate immunity. They have critical functions in organ development, maintenance of tissue homeostasis, and host protection during infection. Macrophages are highly heterogenous cells that can rapidly change their function in response to local microenvironmental signals. Although distinct macrophage subsets with unique functional abilities have been described, it is generally believed that macrophages represent a spectrum of activated phenotypes rather than discrete stable subpopulations (1,2). Fate mapping analyses and lineage tracing experiments have indicated that tissue macrophages in many organs are of early embryonic origin (3–5). Monocytes are a heterogeneous population of myeloid cells that originate from progenitors in the bone marrow and traffic via the bloodstream to peripheral tissues. Monocytes are bone marrow–derived circulating cells that localize to injured and inflamed tissues and differentiate locally into diverse myeloid cell populations (6).

Given the importance of monocyte/macrophage subsets in health and disease, it is critical to identify the mechanism by which these immune cells are specialized. Transcriptional regulation is the major locus that determines cell specialization. Observations obtained from macrophages involved in chronic inflammation, chronic infection, or cancer strongly suggest that the myeloid compartment has a much broader transcriptional repertoire, depending on

the different environmental signals received (7–10). The signal transducer and activator of transcription (STAT), peroxisome proliferator-activated receptor gamma (PPARγ), nuclear factor kappa-light-chain-enhancer of activated B cells (NF-κB), Krüppel-like family (KLF), and GATA6 families of transcription factors have been identified as regulators of monocyte/macrophage diversification (7,8). Nothing is known about the role of GATA3 zincfinger transcription factors in monocyte/macrophage specialization and function in vivo.

GATA3 is required for the differentiation of T helper 2 (Th2) cells, and is therefore regarded as a master regulator for these cells (11). GATA3 also regulates T cell development (12,13), the generation and function of natural killer cells (14), the function of regulatory T cells (15,16), the generation of type 2 innate lymphoid cells (17,18), as well as tumorigenesis (19). Using mouse models of myocardial infarction (MI) or pressure overload, we found that GATA3 plays an important role in the biology of monocytes/macrophages and cardiac pathologies.

METHODS

ANIMAL ETHICS.

All surgical procedures described here were performed in accordance with the National Institute of Health standards and approved by the Institutional Animal Care and Use Committee of Cedars-Sinai Medical Center. Animals were euthanized at the end of each experiment by an overdose of isoflurane (inhalational anesthetic), and death was ensured by physical means, either cervical dislocation or by a pneumothorax that precedes harvest of vital organs. These methods are consistent with recommendations from the panel on euthanasia of the American Veterinary Medical Association.

MOUSE STRAINS.

LysM-Cre mice (004781; B6.129P2-Lyz2tm1[cre]Ifo/J) on a congenic C57BL/6J background were purchased from the Jackson Laboratory (Bar Harbor, Maine). GATA3 floxed ($GATA3^{fl/fl}$) mice (gift from Dr. William E. Paul through the NIAID/Taconic program) are described (20) and bred in-house. Myeloid-specific GATA3–deficient mice were generated by crossing $GATA3^{fl/fl}$ mice with LysM-Cre mice and are designated as mGATA3KO in this paper. Mice were fed a standard rodent chow diet and housed in microisolator cages in a special pathogen-free facility. All litter sizes were normal. Homozygous pups appeared to be healthy and were of normal size and body weight. Blood analysis showed no difference in the level of white blood cells, red blood cells, hemoglobin, and platelets between mGATA3KO mice and control Cre mice. For experiments described in this paper, adult male mice (11 to 12 weeks of age) were used. At this age, developmental growth of the heart is complete. The weight of each mouse at this age ranged between 25 and 30 g. If animals were observed with nonexperimental-related health conditions (i.e., from fighting), they were removed from the study groups. The number of animals in each experimental group is indicated in the tables or figure legends. Detailed genotype analyses of the mGATA3KO mice are included in **Online Figure 1**.

MYOCARDIAL INFARCTION.

Acute MI was induced essentially as described (21,22). After anesthesia with isoflurane (4% induction, 2% maintenance), mice were intubated with polyethylene-50 tubes (Intramedics, Becton-Dickinson, Sparks, Maryland), and connected to a small animal volume control ventilator (Harvard Apparatus, Holliston, Massachusetts). Ventilation was done with a tidal volume of 350 μl at 120 cycles/min. Each mouse was placed in a supine position on a heating table to prevent hypothermia during anesthesia. The heart was then exposed via sternotomy with the use of a small retractor. The heart was positioned so that the left ventricle (LV), aorta, and left atrium were exposed for suture placement. A 7–0 suture was placed in the anterior myocardium to occlude the left anterior descending artery (LAD). The heart was returned to its original position, and a small piece of Seprafilm (Genzyme Biosurgery, Cambridge, Massachusetts) was placed on the surface of the LV to reduce adhesions. The sternum incision was closed with 7–0 sutures, and the skin incision was closed with 4–0 sutures. The endotracheal tube was gently retracted after spontaneous breathing was restored. Relatively large infarctions were induced by proximal ligation (4 mm from the apex), and small infarctions were induced by distal ligation (2 mm from the apex) of the LAD. Some of the mice that survived at the end of 28 days were also used for echocardiographic, hemodynamic, and infarct size analyses, as indicated in each study. The surgeon was blinded to the genotypes of the mice.

TRANSVERSE AORTIC CONSTRICTION.

This procedure was performed essentially as described (23). Male mice were anesthetized, and the abdominal aorta was opened at the suprarenal level. The aorta was constricted by placing 9–0 silk sutures around the aorta with the help of a 28-G needle. At the indicated times after constriction, cardiac function and blood pressure (BP) were measured. The mice were euthanized and their tissues were harvested for further analysis. All baseline data were collected before transverse aortic constriction (TAC).

ECHOCARDIOGRAPHY.

Transthoracic echocardiography was performed while the animals were anesthetized by isoflurane (2% induction and 1.5% maintenance). Two-dimensional short- and long-axis images of the LV were obtained at the papillary muscle level (Vevo 770, Visual Sonics, Toronto, Ontario). The following parameters were measured: ejection fraction; fractional shortening; left ventricular internal diameter diastolic; left ventricular internal diameter systolic; posterior wall thickness diastolic; and posterior wall thickness systolic. Three consecutive cardiac cycles were analyzed, and the average was used for data analysis. Two different time points were selected for echocardiographic studies: pre-TAC baseline and 2 months post-TAC.

BP MEASUREMENTS.

BP was measured using a tail cuff CODA 6 system from Kent Scientific (Torrington, Connecticut). Thoracic BP proximal to the constricted site was calculated by adding tail BP to the Doppler-derived BP gradient across the constriction. Multiple recordings were performed to obtain mean data.

HISTOLOGICAL ANALYSIS OF MURINE HEARTS.

Mice of each genotype were weighed, and hearts were harvested, rinsed in phosphate-buffered saline, and weighed at the indicated times after MI or TAC. Hearts were cut in a cross section just below the level of the papillary muscle. The top half of the heart was formalin-fixed and embedded in optimal cutting temperature compound (Fisher Healthcare, Waltham, Massachusetts). Five-micron sections were prepared at 200-μm intervals. Sections were stained with hematoxylin and eosin for examination of gross appearance, and Masson's trichrome and periodic acid–Schiff with hematoxylin (PASH) were used to facilitate quantification of fibrosis and cardiomyocyte size, respectively. Cardiac fibrosis was determined by calculating the percentage of the Masson's trichrome–stained area of interstitial fibrosis per total area of cardiac tissue. Cardiomyocyte hypertrophy was assessed by measuring the cross-sectional area of 100 cardiomyocytes per PAS-H–stained section in 10 randomly-selected fields having nearly circular capillary profiles and centered nuclei in the LV free wall. Inflammatory cells were detected using the rat anti-mouse monoclonal immunoglobulin G (IgG) monocyte/macrophage marker (Mac-2, Cedarlane Laboratories, Burlington, Ontario) followed by biotinylated rabbit anti-rat IgG, with visualization using the VECTASTAIN Elite ABC Kit (Vector Laboratories, Burlingame, California). Positively-stained cells per cross section were manually counted in 3 sections per heart. The anti-GATA3 antibody (clone D-16; sc-22206, Santa Cruz Biotechnology, Dallas, Texas) was used for GATA3 staining. For immunofluorescent staining, LV sections from Cre mice subjected to MI for 8 days were stained with fluorescent-labeled antibodies. Images were captured and analyzed by the Confocal Imaging Core at Cedars-Sinai Medical Center. Histological images were analyzed using ImagePro Version 4.1 software (Media Cybernetics, Inc., Rockville, Maryland). Blinded measurements were made by 2 independent observers. A list of all antibodies used in immunostaining and fluorescent immunostaining is included in **Online Table 1**.

FLOW CYTOMETRY

Hearts were extensively flushed with phosphate-buffered saline, and LVs were excised, minced with scissors, and digested in collagenase I (450 U/ml), collagenase XI (125 U/ml), DNase I (60 U/ml), and hyaluronidase (60 U/ml) (Sigma-Aldrich, St. Louis, Missouri) at 37°C for 1 h. LVs were subsequently homogenized through a 40-μm cell strainer.

Cell viability was determined by incubating cells with LIVE/DEAD Fixable Blue Dead Cell Stain single-color dyes (Invitrogen, Carlsbad, California) for 30 min at room temperature. After 1 rinse with washing buffer, cells were incubated with CD16/32 antibody (BioLegend, San Diego, California) at 4°C for 15 min to block nonspecific binding of immunoglobulin to the Fc receptors. Cells were then labeled with the following rat anti-mouse antibodies from BioLegend: PE-labeled anti-CD45, PE-Cy7–labeled anti-CD11b; Brilliant Violet 421-labeled anti-F4/80; PerCP-Cy5.5–labeled anti-Ly6G; Alexa Fluor 700-labeled anti-Ly6C from BD Pharmingen (San Jose, California); and APC-labeled anti-CCR2 from R&D Biosystems (Minneapolis, Minnesota). Cells were washed twice, resuspended in staining buffer, and immediately recorded with a Becton Dickinson LSR Fortessa (BD Biosciences) at the Flow Cytometry Core of Cedars-Sinai Medical Center. Data were analyzed with

Summit V4.3 software (Dako Colorado, Fort Collins, Colorado). Only singlet cells were analyzed. All doublets were excluded from the analysis by monitoring the SSC/FSC pulse width channel. All antibodies used in flow cytometry experiments are listed in **Online Table 1**.

MILLIPLEX MOUSE CYTOKINE/CHEMOKINE ASSAY.

Biomarker analyses of mouse sera (before MI, 2, 8, and 28 days post-MI) were performed by the Immune Assessment Core Facility at the University of California–Los Angeles using the multiplex assay. The Milliplex Mouse Cytokine/Chemokine 32-Plex Magnetic Bead Kit (EMD Millipore, Burlington, Massachusetts) was used as per the manufacturer's instructions. Plasma samples were prepared with a 2-fold dilution: 25 μl of the diluted plasma samples were mixed with 25 μl of magnetic beads and incubated overnight at 4°C while shaking. After washing the plates with wash buffer in a Biotek ELx405 washer (BioTek Instruments, Winooski, Vermont), 25 μl of a biotinylated detection antibody was added, and plates were incubated for 1 h at room temperature while shaking. This was followed by the addition of 25 μl of the streptavidin-phycoerythrin conjugate to the reaction mixture and incubation of the plates for another 30 min at room temperature while shaking. Following additional washes, beads were resuspended in sheath fluid, and fluorescence was quantified using a Luminex 200 instrument (Luminex Corporation, Austin, Texas). Data were analyzed using MILLIPLEX Analyst 5.1 Software.

QUANTITATIVE REAL-TIME POLYMERASE CHAIN REACTION.

Total RNA was extracted from the lower half of the LV using TRIzol (Invitrogen). After DNase treatment, 500 ng of total RNA were reverse transcribed using the High-Capacity cDNA Archive Kit (Applied Biosystems, Foster City, California). RNA primers for each gene were designed using Primer3 software program. Gene expression was determined by qPCR using Bio-Rad SsoFast EvaGreen Supermix (Bio-Rad Laboratories, Hercules, California). Glyceraldehyde 3-phosphate dehydrogenase (GAPDH) was used as an internal control. There were no significant differences in GAPDH expression levels by genetic background or treatment. Reactions were run on an iQ5 machine (BIO-RAD) with analysis software. Threshold cycles (C_T) were determined by an inprogram algorithm assigning a fluorescence baseline based on readings before exponential amplification. Fold change in expression was calculated using the 2^{-ddCr} method. GAPDH abundance was used for normalization. Results are represented as mean fold changes relative to sham-operated or GAPDH expression. Each experiment was repeated 3 times, and each sample was run in triplicate. The results shown are the mean of triplicate determinations ± SD. Primer sequences are listed in **Online Table 2**.

WESTERN BLOT.

Cultured cells were lysed with boiling sample buffer. Protein determination was made using the Bio-Rad Protein Assay. An equal amount of proteins was loaded into each lane of a sodium dodecyl sulfate–polyacrylamide gel, followed by transfer to nitrocellulose paper. After transfer was completed, the paper was blocked with blocking solution (1% TWEEN 20

and 1% powdered milk), incubated with the appropriate antibodies, and developed. A list of the antibodies used can be found in **Online Table 1**.

STATISTICS.

Statistical analysis was performed using GraphPad Prism Software (Version 4.0, GraphPad, La Jolla, California). In this comparative study, we compared cardiac functions and phenotype of control Cre mice with mGATA3KO mice before and after the 2 procedures. Following MI, the phenotype of cells in each group is determined by flow cytometry in the LV digest of each mouse. We used the independent parametric Student *t*-test to compare the 2 groups. In this analysis, we used the unpaired Student *t*-test with the assumption that either both groups have the same SD or with the Welch's correction, which does not assume equal SDs. The results were similar; therefore, we have shown data without the Welch's correction. A p value < 0.05 was considered statistically significant.

The number of animals were based on power calculations, published reports, and our experience. The power analysis for the number of mice necessary for in vivo experiments is based on 80% power and an alpha of 0.05.

RESULTS

DEFICIENCY OF GATA3-POSITIVE MACROPHAGES IMPROVED CARDIAC FUNCTION.

Monocytes/macrophages promote the process of myocardial healing after MI, as depletion of these cells drastically impairs healing and exacerbates disease outcomes (24,25). These cells are highly heterogeneous and display a high degree of plasticity. It is unclear which subtype of monocytes/macrophages promotes healing and which impairs tissue repair in vivo. We used 2 established animal models of cardiac injury to assess the function of GATA3sufficient and GATA3-deficient macrophages in the pathogenesis of cardiac diseases. In the first animal model, MI was induced by ligation of the coronary artery. In the second animal model, the aorta was constricted to induce pressure overload. Cardiac function and remodeling in the myeloid-specific GATA3-deficient mice and the GATA3-sufficient control Cre mice were compared.

MI MODEL.

We first determined the distribution of GATA3-positive cells in the myocardium of control mice before and after MI by immunohistochemical analysis of LV sections. Few, if any, GATA3-positive cells were detected in the LVs of control mice before MI (not shown). After MI, however, a large number of GATA3-positive cells accumulated in the macrophage-rich region of the myocardium (**Figure 1A**), but not in the healthy region, indicating that GATA3-positive cells were largely localized to the ischemic region of the myocardium. To demonstrate GATA3 expression by macrophages, we costained LV sections with fluorescentlabeled antibodies for macrophages (CD11b, red) and GATA3 (green). 4′,6-Diamidino-2phenylindole (DAPI) was used to stain nuclei (**Online Figure 2**). The merged confocal image shows that GATA3 protein is localized to the nuclei of macrophages in the infarcted region (**Figure 1A**). Collectively, these data show that GATA3-positive macrophages are not found in the normal LV, but they appear after MI.

Next, we compared cardiac function in the 2 mouse genotypes before and 28 days after MI. We found no significant differences in cardiac function between the 2 mouse genotypes before MI (baseline) (**Table 1**). After MI, however, there were significant differences in cardiac function between the 2 mouse genotypes, as indicated by the echocardiographic analysis (**Figure 1B)** and pooled data (**Table 1**). These analyses revealed that, compared with the control group, mice with the GATA3 deficiency in myeloid cells were protected against post-MI events, showing less ventricle dilation and greater preservation of contractile function. Similarly, analysis of the morphology of the harvested hearts showed the presence of more myocardium in mGATA3KO mice compared with the control group (**Figure 1C**). As sections closer to the highly ischemic apex areas were examined, differences between the 2 heart genotypes became more apparent, with mGATA3KO hearts having more myocardium mass and less fibrosis compared with control hearts (**Figure 1C**). Following harvest, we measured the scar area, the risk area, the viable myocardium, and the infarct wall thickness in the 2 genotype groups. The scar area was significantly smaller and the viable myocardium and infarct wall thickness were significantly higher in the mGATA3KO group compared with the control group (**Figure 1D**). Morphology of all of the harvested hearts is shown in **Online Figure 3**.

PRESSURE OVERLOAD MODEL.

Each tissue exhibits distinct characteristics of inflammation as a result of general and local molecular, immunologic, and physiological processes. We (23) and others (26) have previously shown that infiltration of macrophages contributes to remodeling of the pressure-overloaded mouse heart. We used this animal model to ask whether the improvement of cardiac function after MI in the mGATA3KO mouse is contextspecific or independent of the ischemic milieu. Serial 2-dimensional echocardiographic analysis of heart function at 2 months following pressure overload demonstrated that all of the cardiac hypertrophy parameters were significantly improved in mGATA3-deficient mice compared with the control group **(Figure 2A and Table 2**).

To further analyze the effect of macrophage-specific GATA3 deficiency on cardiac hypertrophy, hearts were harvested at 2 months post-TAC, and the heart weight to body weight ratio (HW/BW) was calculated. Additionally, histochemical analysis was performed to determine the size of cardiomyocytes and collagen content. The HW/BW ratio was significantly lower in mGATA3KO mice compared with the control group (**Table 2**). Similarly, cardiac myocyte size and collagen content were significantly higher in the control group compared with mGATA3KO mice (**Figure 2B**). In addition, the level of other markers of cardiac hypertrophy were significantly improved in mGATA3KO mice compared with control mice **(Online Figure 4)**. Thus, depletion of GATA3-positive macrophages attenuated cardiac hypertrophy in response to pressure overload. Together, the in vivo functional data suggest that the absence of GATA3positive macrophages improve cardiac function and that this improvement is independent of the ischemic microenvironment.

PHENOTYPE OF MONOCYTES/MACROPHAGES IN THE LV OF THE 2 MOUSE GENOTYPES.

We analyzed the composition of monocytes/macrophages before and after ischemic injury in the 2 mouse genotypes in order to determine the cellular mechanism by which GATA3-

positive macrophages influence cardiac function. LVs were harvested and digested with a cocktail of proteases. The single-cell population was stained with the appropriate antibodies, and the labeled cells were analyzed by flow cytometry (23,27). The gating strategy for flow cytometric analysis of the samples is outlined in **Online Figure 5**. We found no significant differences in the level of neutrophils between the 2 mouse genotypes at baseline (**Figure 3A**). In both mice genotypes, the level of neutrophils was significantly increased 2 days after MI compared with the baseline. Between the 2 mouse genotypes, the level of neutrophils was significantly lower in mGATA3KO mice compared with the control mice at 2 days post-MI (**Figure 3A**). Although the level of total monocytes/macrophages were similar between the 2 mouse genotypes at baseline, the level was significantly increased after MI in both mouse genotypes. The level of total monocytes/macrophages was significantly lower in mGATA3KO mice compared with the control group at both 2 and 8 days following MI (**Figure 3A**).

Recruitment of monocytes into the infarcted myocardium depends on CCR2 signaling (28, 29). The $CCR2^{+}$ monocyte subset displays higher migratory and infiltration capacity than the $CCR2^{-}$ subset and is considered the murine inflammatory monocyte (30). The recruited $CCR2^{+}$ cells are derived from hematopoiesis, whereas most $CCR2^{-}$ cardiac macrophages are derived from yolk sac progenitors (31,32). The levels of the total $CCR2^{+}$ and $CCR2^{-}$ monocyte/macrophage subsets were similar between the 2 mouse genotypes at baseline; however, at 8 days after MI, the level of CCR2 monocytes was significantly higher in both genotypes (**Figure 3B**). This suggests that the improvement of cardiac function is not related to the presence of fewer proinflammatory monocytes in the infarcted myocardium of mGATA3KO mice.

In the context of MI, 2 subpopulations of monocytes are thought to be sequentially recruited into the myocardium. $Ly6C^{hi}$ monocytes, have a short life span of only 20 h and infiltrate the myocardium as early as 30 min after MI (29,33,34). This is followed by recruitment of $Ly6C^{lo}$ cells, which accumulate during the reparative phase that can persist for several weeks, and renew partially through proliferation (35). $Ly6C^{hi}$ monocytes differentiate from $Ly6C^{hi}$ progenitors, whereas the reparative $Ly6C^{lo}$ cells differentiate from $Ly6C^{hi}$ monocytes (3,36). Embryonic cardiac macrophages disappear shortly after MI (37), suggesting that $Ly6C^{lo}$ macrophages in the infarct zone are most likely derived from $Ly6C^{hi}$ monocytes.

The frequency of the 2 Ly6C cell subsets was similar between the 2 mouse genotypes at baseline (**Figure 3C**). After MI, however, the level of total $Ly6C^{hi}$ cells increased in both mouse genotypes at 2 days post-MI and then declined to normal levels at 8 days post-MI. Compared with the control group, the level of total $Ly6C^{hi}$ cells was significantly higher in the mGATA3KO mice at 8 days post-MI (**Figure 3C**). Further analysis of the $Ly6C^{hi}$ subset of monocytes/macrophages (CCR2+/Ly6Chi and $CCR2^{-}/Ly6C^{hi}$) showed that although the levels of $CCR2^{+}/Ly6C^{hi}$ and $CCR2^{-}/Ly6C^{hi}$ cell subsets seemed to be lower in the mGATA3KO group, they did not demonstrate a statistically significant difference from the control group (**Figure 3D**). After MI, however, the level of proinflammatory $CCR2^{+}/Ly6C^{hi}$ cells in the mGATA3KO group was significantly higher than in the control group (**Figure**

3D). The level of CCR2^{-}/Ly6C^{hi} cells was similar between the 2 mouse genotypes before and after MI.

With respect to the total level of Ly6C^{lo} cell subsets (CCR2^{+} /Ly6C^{lo} and CCR2^{-} /Ly6C^{lo}), we found no significant differences between the 2 genotype groups at baseline (**Figure 3E**). After MI, however, the level of CCR2^{-} /Ly6C^{lo} macrophages were significantly lower in mGATA3KO mice compared with control mice (**Figure 3E**). Statistical analysis revealed that the level of the Ly6C cell subset significantly increased at 2 days post-MI ($p = 0.01$), followed by a significant reduction at day 8 ($p = 0.002$) in the control Cre mouse group. Among the mGATA3KO groups, the level of CCR2^{-}/Ly6C^{lo} cells were significantly reduced at 2 days ($p = 0.0009$) and 8 days ($p = 0.003$) post-MI (**Figure 3E**). Comparison of the 2 mouse genotypes showed that the level of CCR2^{-}/Ly6C^{lo} macrophages was significantly lower in the mGATA3KO group after MI compared with the control group. Taken together, these results suggest that the improvement of cardiac function in the mGATA3KO mouse is associated with the presence of many proinflammatory macrophages, but few anti-inflammatory cells when compared with the control mouse.

PHENOTYPE OF MONOCYTES IN THE PERIPHERAL BLOOD OF THE 2 MOUSE GENOTYPES.

Peripheral blood monocytes appear to be the major contributor to the macrophage pool in the acute phase of MI (38). They are primarily recruited from the spleen (39,40). We found no significant differences in the level of peripheral blood neutrophils and total monocytes between the 2 mouse genotypes (**Online Figure 6**). After MI, the level of total monocytes was significantly increased in the control group compared with the mGATA3KO group at 2 days post-MI. With respect to the monocyte subsets, at 8 days post-MI, levels of proinflammatory monocytes (total Ly6C^{hi} and CCR2^{+} /Ly6C^{hi}) were higher in the peripheral blood of mGATA3KO mice compared with the control group (**Figure 4A**). With respect to the level of anti-inflammatory monocytes (total Ly6C^{hi} and CCR2^{-}/Ly6C^{hi}) the level of total Ly6C and CCR2^{-}/Ly6C^{lo} cell subsets were significantly increased at 2 and 8 days post-MI among the control group (**Figure 4B**), whereas the level of these cells among the mGATA3KO group was significantly reduced (**Figure 4B**). Between the genotype groups, the level of total Ly6C^{lo} and CCR2^{-}/Ly6C^{lo} cell subsets were significantly higher in the mGATA3KO group compared with the control group at baseline, and the level of these cells was significantly reduced at 8 days postMI. Collectively, the pooled flow cytometry data indicate that in the mGATA3KO mouse group, the level of proinflammatory macrophages was significantly higher, whereas the frequency of the anti-inflammatory cells were significantly lower compared with the control group.

ANALYSIS OF SERUM PROTEINS FROM THE 2 MOUSE GENOTYPES.

Various growth factors and cytokines secreted by myeloid cells coordinate various stages of the wound healing process (41). To assess the systemic effect of deficiency of GATA3-positive macrophages, we determined the serum concentration of various growth factors and cytokines from the 2 mouse genotypes before and at the indicated times after MI. Multiplex analysis of serum proteins showed no major differences in the profile of serum growth

factors and cytokines between the 2 mouse genotypes before and after MI (**Online Figure 7**). This suggests that the effect of the GATA3-positive cells is most likely regional.

MECHANISM OF GATA3 EXPRESSION IN MACROPHAGES.

To demonstrate the ability of macrophages to express GATA3, we used cultured cells. The $CCR2^{+}/Ly6C^{hi}$ proinflammatory and $CCR2^{-}/Ly6C^{lo}$ resident monocytes/macrophages are generally thought to preferentially differentiate into M1 inflammatory and M2 anti-inflammatory macrophages, respectively, during early inflammation (42,43). Interferon (IFN)γ-activated cells represent classically-activated macrophages (M1), whereas interleukin (IL)-4 activated cells, represent alternatively- activated macrophages (M2) (44–46).

First, we asked about the phenotype of GATA3-positive macrophages. To explore this, we used both peritoneal and bone marrow-derived macrophages because their responses to the agonists are different (47,48). Peritoneal or bone marrow cells from control mice were harvested, cultured, and then treated with IFNγ or IL-4 for the indicated times. qPCR analyses of total RNA showed that IL-4, but not IFNγ, induced GATA3 expression in both peritoneal and bone marrow-derived macrophages (**Figure 5A**). The induction peaked at 2 h and declined thereafter, reaching the untreated level at 8 h post-treatment. The qPCR data were further validated by western blot analysis of the cultured cells (**Figure 5B**). Similar results were found in RAW264.7 and J744a mouse macrophage cell lines (not shown). These results suggest that GATA3 expression is rapidly and transiently induced by IL-4. The induction of GATA3 by IL-4 in cultured macrophages was found to be dose-dependent (**Figures 5C and 5D**). Finally, to demonstrate GATA3 localization within macrophages, bone marrow-derived macrophages were cultured on the slide chamber, treated with IL-4 for 4 h, fixed, and costained with fluorescentlabeled anti-CD11b (**Figure 5E, red**) and anti-GATA3 (**Figure 5E, green**) antibodies. DAPI was used to stain the nucleus. GATA3-positivity was found in macrophage nuclei (**Figure 5E, merge**). Collectively, these results indicate that GATA3 is not expressed in resting macrophages, but is induced by IL-4, suggesting that GATA3-positive macrophages display a M2 polarized phenotype.

GATA3 encodes 2 transcripts that differ in their alternative, untranslated, first exon. IL-4 initiates and establishes GATA3 transcription in developing Th2 cells from the distal promoter, encoding a larger transcript, whereas the proximal promoter remains silent (49). Nothing is known about GATA3 transcript expression in macrophages. To identify which GATA3 transcript is induced by IL-4 in macrophages, peritoneal macrophages were treated with IL-4, and expression of the GATA3 transcripts was assessed by qPCR using primers specific to the distal (E1a) or proximal (E1b) promoters. We found that IL-4 treatment rapidly induced GATA3 expression from the proximal promoter, peaking at 2 h, and then declining to control levels at 24 h after treatment (**Figure 5F**). Unlike T cells, the distal promoter remained silent in the macrophages. Therefore, the expression of the GATA3 transcript in macrophages seems to be different than in T cells.

Macrophage polarization is a dynamic event that adapts to changes in the cytokine milieu. To identify which growth factors and cytokines induce GATA3 expression in macrophages, cultured bone marrow–derived macrophages were treated with the indicated cytokines, and

GATA3 expression was evaluated by qPCR. We found that, except for IL-4, other factors did not induce GATA3 expression (**Figure 5G**), suggesting that the induction of GATA3 in macrophages is specific to IL-4.

Sterile inflammation is a major component of tissue injury and fibrosis. Synthesis of wound collagen is dependent on the availability of the amino acids proline and hydroxyproline (50). These amino acids are synthesized within the extracellular wound fluid through conversion of arginine to ornithine, a metabolic precursor of proline (51), by arginase-1 (Arg-1), which is expressed by wound macrophages (52,53). We hypothesized that the lower level of cardiac fibrosis in the infarcted myocardium of mGATA3KO mice may be related to lower levels of Arg-1. To explore this, cultured bone marrow–derived macrophages isolated from the 2 mouse genotypes were treated with IFNγ or IL-4, and expression of Arg-1 was measured by qPCR and western blot (**Figure 5H**). Both assays showed that addition of IL-4, but not IFNγ, markedly induced Arg-1 expression in control macrophages, whereas the level of response was markedly attenuated in macrophages derived from mGATA3KO mice (**Figure 5G**). This is consistent with the notion that GATA3-sufficient macrophages display the M2 phenotype.

Finally, we asked whether factors that induce GATA3 in cultured macrophages are found in the infarcted myocardium. To explore this, LV sections from the 2 mouse genotypes were stained with the anti-IL-4 antibody. Additionally, LV sections were stained with the anti-IL-33 antibody because this cytokine was reported to induce GATA3 in macrophages (**54**). Immunostaining analysis of sections from the normal control mice stained with anti-IL-4 or antiIL-33 antibodies showed that these cytokines are not expressed under the stationary state condition in the myocardium (not shown). However, strong staining of the 2 cytokines was detected in the acute MI sections, localized in the macrophage-rich region of the infarcted myocardium (**Figure 5I**). Immunostaining of sections from the normal mGATA3KO mice showed no positive staining (not shown). However, weak IL-33 staining that colocalized with the macrophages was detected in the infarcted myocardium (**Figure 5J**). Unlike the control mice, we did not detect IL-4 positive staining in the infarcted myocardium of mGATA3KO mice (**Figure. 5J**), suggesting that IL-4 expression in the infarcted myocardium is dependent on the presence of GATA3-positive macrophages. These results suggest that IL-4 or IL-33 are induced after MI and may be responsible for the appearance of GATA3-positive macrophages in the myocardium.

DISCUSSION

The GATA3 transcription factor is known as a master regulator of T-cell polarization. However, its role in regulation of the macrophage phenotype remains unknown. We found that GATA3-positive macrophages are not found in the normal heart; however, they accumulate in the myocardium after acute MI. As monocytes are the major source of myocardial macrophages in acute MI (37), monocyte-derived macrophages are the most likely source of GATA3-positive cells. To understand the role of this macrophage subset in the pathogenesis of cardiac diseases, we generated myeloid-specific GATA3-deficient mice and compared the cardiac function of mGATA3KO mice and control Cre mice. We noted that the absence of GATA3-myeloid cells led to a significant improvement of cardiac

function after MI. This improvement appeared to be independent of the ischemic microenvironment, as the cardiac function and remodeling of mGATA3KO mice were significantly improved in response to pressure overload. Our data suggest that GATA3-positive macrophages do not contribute to the normal physiology of the heart; however, their presence in the stressed heart exacerbates the pathology.

Monocytes recruited to the infarcted myocardium are thought to be critical for myocardial remodeling after MI. Monocytes produced in the bone marrow and spleen enter the blood after MI and are recruited to the injured myocardium in 2 phases (33,39) that are also likely to occur in humans (55). The first phase is dominated by $Ly6C^{hi}$ proinflammatory monocytes and the second phase by $Ly6C^{lo}$ "reparative" monocytes/macrophages. We hypothesized that the improvement of cardiac function in mGATA3KO mice results, in part, from the presence of fewer proinflammatory monocytes/macrophages in the ischemic myocardium. However, analysis of the phenotype of the macrophages in the infarcted myocardium did not support this notion. We found that the total level of bone marrow–derived $CCR2^{+}$ monocytes/macrophages is significantly higher in mGATA3KO mice at 2 days post-MI compared with the control group. In addition, the total level of $Ly6C^{hi}$ and $CCR2^{+}/Ly6C^{hi}$ proinflammatory cell subsets were significantly higher in the myocardium of mGATA3KO mice after MI. Furthermore, the level of total $Ly6C^{hi}$ and $CCR2^{+}/Ly6C^{hi}$ cells in peripheral blood of mGATA3KO mice was significantly higher than in the control group. Collectively, these results suggest that the improvement of cardiac function after MI in mGATA3KO mice is not the result of fewer proinflammatory macrophages in the myocardium. This was unexpected because the persistence of proinflammatory macrophages is thought to be responsible for maladaptive remodeling after MI or in response to pressure overload (56). Although targeting of proinflammatory pathways is thought to be an important strategy to control excess tissue fibrosis, numerous anti-inflammatory drugs, including corticosteroids, have been found to have little or no therapeutic benefit in idiopathic pulmonary fibrosis or other diseases.

In most injured mouse tissues, including the myocardium (33), kidney (57), muscle (58), and lung (59,60), infiltration of proinflammatory cells is followed by a decline in their numbers with a concomitant increase of $Ly6C^{lo}$ cells. We found that the frequency of $Ly6C^{lo}$ cells, both the total $Ly6C^{lo}$ and $CCR2^{-}/Ly6C^{lo}$ cell subsets, was lower in the ischemic myocardium of mGATA3KO mice compared with control mice. In the peripheral blood of mGATA3KO mice, the level of $Ly6C^{lo}$ cell subsets either remained unchanged or was reduced after MI. Thus, fewer numbers of the reparative macrophage subset are found in mGATA3KO mice, and this may be responsible for the improvement in cardiac function after MI. This notion is further supported by the pressure overload cardiac hypertrophy model. We found that the absence of GATA3-positive macrophages resulted in improvement of cardiac function. Using this animal model, the number of $Ly6C^{lo}$ macrophages was reported to increase after pressure overload in the wild type C57BL/6 mouse and remain elevated, whereas the number of $Ly6C^{hi}$ proinflammatory macrophages remained unchanged (61). The investigators suggested that the increased level of $Ly6C^{lo}$ macrophages, but not $Ly6C^{hi}$ cells, is responsible for the maladaptive remodeling of the myocardium in response to pressure overload. $Ly6C^{lo}$ cells are also reported to be associated with the fibrosis phase, but not the inflammation phase, of lung fibrosis (62). Collectively, these results suggest that

targeting the Ly6C^{lo} macrophages may be a useful strategy to control excessive myocardial fibrosis.

Although initial fibrosis after MI promotes the healing process, excessive fibrosis leads to maladaptive remodeling and heart failure (63,64). Macrophages control tissue fibrosis through expression of various cytokines, chemokines, and molecules that regulate turnover of the extracellular matrix. We noted that the absence of GATA3-positive macrophages attenuates myocardial fibrosis in the 2 cardiac injury models. In cultured macrophages, GATA3 is specifically induced by IL-4. Although the contribution of IL-4 to fibrosis varies in different diseases (65), it is considered a potent fibrotic mediator, as it is nearly twice as effective as transforming growth factor beta in inducing collagen synthesis from human skin-derived fibroblasts (66). Histochemical analysis of MI sections also showed strong expression of IL-4 and IL-33 in the infarct region, colocalizing with macrophages, suggesting that these cytokines may be responsible for GATA3 expression in macrophages in vivo. IL-33 is a highly fibrogenic cytokine (67), and it induces M2 polarization of macrophages as well as promotion of lung fibrosis (68,69). In the human heart, M2 macrophages are associated with cardiac fibrosis in the ischemic heart (70). These data suggest that the M2 macrophage phenotype may be associated with the enhanced fibrosis rather than the proinflammatory M1 phenotype.

Induction of GATA3 in macrophages seems to be different than in T cells. In macrophages, GATA3 expression in response to IL-4 is transient peaking at 2 h after treatment, and rapidly declines to control levels thereafter. In contrast, GATA3 expression is slow and longlasting, as GATA3 mRNA levels are significantly increased after 18 h of IL-4 treatment of T cells, and the message level remains elevated for at least 48 h (49). The second difference relates to promoter usage. The GATA3 gene encodes 2 transcripts that differ in their alternative, untranslated first exons. In developing T cells, GATA3 is induced by IL-4 through activation of the distal promoter (49). In contrast, we noted that the induction of GATA3 expression by IL-4 in macrophages is mediated by the proximal promoter whereas the distal promoter remains inactive.

CONCLUSIONS

We found that GATA3-positive macrophages accumulated rapidly in the infarcted region of the myocardium and colocalized with macrophages. Analysis of cardiac function in mGATA3KO mice showed that the absence of GATA3-positive cells led to a significant improvement in cardiac function in response to MI or pressure overload. Analysis of myocardial macrophages after MI showed that this improvement was associated with the accumulation of fewer reparative Ly6C^{lo} macrophages, but not proinflammatory Ly6C^{hi} monocytes. Analysis of cultured macrophages showed that IL-4 rapidly and transiently induces GATA3 by a different mechanism than in T cells. Our data suggest that targeting GATA3 signaling in macrophages may be a useful strategy for developing immunotherapeutic approaches to treat cardiac diseases.

LIMITATIONS OF OUR STUDY.

The limitations of our investigation are at least 2-fold. First, to generate myeloid-specific GATA3-deficient mice, the GATA3$^{fl/fl}$ mouse is crossed with the widely-used LysM-Cre mouse. As LysM is expressed in all myeloid cells, GATA3 is therefore deleted in all myeloid cells. Thus, the effect of GATA3 deletion on cardiac function is not limited to macrophages. As the role of monocytes/macrophages in the pathogenesis of cardiovascular diseases is well established, we concentrated our efforts on the function of GATA3 deletion in these cells. Second, LysM is expressed in both resident and recruited macrophages. However, its level of expression is higher in the resident macrophages compared with the recruited monocytes (71). Consequently, the deletion of GATA3 is most likely more concentrated in resident macrophages than in recruited monocytes. Therefore, it is likely that the effect of GATA3 deletion on recruited cells, such as monocytes, may be underestimated.

Supplementary Material

Refer to Web version on PubMed Central for supplementary material.

Acknowledgments:

The authors thank Moshe A. Arditi and David Underhill for critically reviewing the manuscript, Cedars Sinai Vivarium personnel for assistance with mouse colony management, and Patricia Lin at the Cedars-Sinai Flow Cytometry Core Facility for her assistance with flow cytometry analysis. In addition, the authors appreciate the UCLA core facility performance of the MILLIPLEX mouse cytokine/chemokine assay. Myeloid-specific GATA3–deficient mice are available from Cedars-Sinai under a material transfer agreement. This work was supported by NIH grant R01 HL104068. The authors gratefully acknowledge the support of the Heart Foundation, the Eisner Foundation, the Spielberg Foundation, the Corday Foundation, the Petersen Foundation, and the Skirball Foundation.

ABBREVIATIONS AND ACRONYMS

Arg-1	arginase-1
BP	blood pressure
HW/BW	heart weight to body weight ratio
LV	left ventricle
mGATA3KO	myeloid-specific GATA3 knockout mouse
MI	myocardial infarction
qPCR	quantitative real-time polymerase chain reaction
TAC	transverse aortic constriction

REFERENCES

1. Murray PJ, Wynn TA. Protective and pathogenic functions of macrophage subsets. Nat Rev Immunol 2011;11:723–37. [PubMed: 21997792]
2. McNelis Joanne C, Olefsky Jerrold M. Macrophages, immunity, and metabolic disease. Immunity 2014;41:36–48. [PubMed: 25035952]

3. Schulz C, Perdiguero EG, Chorro L, et al. A lineage of myeloid cells independent of Myb and hematopoietic stem cells. Science 2012;336:86–90. [PubMed: 22442384]
4. Yona S, Kim K-W, Wolf Y, et al. Fate mapping reveals origins and dynamics of monocytes and tissue macrophages under homeostasis. Immunity 2013;38:79–91. [PubMed: 23273845]
5. Hashimoto D, Chow A, Noizat C, et al. Tissue-resident macrophages self-maintain locally throughout adult life with minimal contribution from circulating monocytes. Immunity 2013;38:792–804. [PubMed: 23601688]
6. Geissmann F, Manz MG, Jung S, Sieweke MH, Merad M, Ley K. Development of monocytes, macrophages, and dendritic cells. Science 2010;327:656–61. [PubMed: 20133564]
7. Mosser DM, Edwards JP. Exploring the full spectrum of macrophage activation. Nat Rev Immunol 2008;8:958–69. [PubMed: 19029990]
8. Lawrence T, Natoli G. Transcriptional regulation of macrophage polarization: enabling diversity with identity. Nat Rev Immunol 2011;11:750–61. [PubMed: 22025054]
9. Xue J, Schmidt SV, Sander J, et al. Transcriptome-based network analysis reveals a spectrum model of human macrophage activation. Immunity 2014;40:274–88. [PubMed: 24530056]
10. Glass CK, Natoli G. Molecular control of activation and priming in macrophages. Nat Immunol 2016;17:26–33. [PubMed: 26681459]
11. Zhu J Transcriptional regulation of Th2 cell differentiation. Immunol Cell Biol 2010;88:244–9. [PubMed: 20065998]
12. Ting CN, Olson MC, Barton KP, Leiden JM. Transcription factor GATA-3 is required for development of the T-cell lineage. Nature 1996;384:474–8. [PubMed: 8945476]
13. Pai SY, Truitt ML, Ho IC. GATA-3 deficiency abrogates the development and maintenance of T helper type 2 cells. Proc Natl Acad Sci U S A 2004;101:1993–8. [PubMed: 14769923]
14. Samson SI, Richard O, Tavian M, et al. GATA-3 promotes maturation, IFN-gamma production, and liver-specific homing of NK cells. Immunity 2003;19:701–11. [PubMed: 14614857]
15. Wang Y, Su MA, Wan YY. An essential role of the transcription factor GATA-3 for the function of regulatory T cells. Immunity 2011;35:337–48. [PubMed: 21924928]
16. Wohlfert EA, Grainger JR, Bouladoux N, et al. GATA3 controls Foxp3$^+$ regulatory T cell fate during inflammation in mice. J Clin Invest 2011;121:4503–15. [PubMed: 21965331]
17. Hoyler T, Klose CSN, Souabni A, et al. The transcription factor GATA-3 controls cell fate and maintenance of type 2 innate lymphoid cells. Immunity 2012;37:634–48. [PubMed: 23063333]
18. Mjösberg J, Bernink J, Golebski K, et al. The transcription factor GATA3 is essential for the function of human type 2 innate lymphoid cells. Immunity 2012;37:649–59. [PubMed: 23063330]
19. Sanda T, Lawton LN, Barrasa MI, et al. Core transcriptional regulatory circuit controlled by the TAL1 complex in human T cell acute lymphoblastic leukemia. Cancer Cell;22:209–21. [PubMed: 22897851]
20. Zhu J, Min B, Hu-Li J, et al. Conditional deletion of *Gata3* shows its essential function in T_H1-T_H2 responses. Nat Immunol 2004;5:1157–65. [PubMed: 15475959]
21. Oh YS, Thomson LEJ, Fishbein MC, Berman DS, Sharifi B, Chen PS. Scar formation after ischemic myocardial injury in MRL mice. Cardiovasc Pathol. 2004;13:203–6. [PubMed: 15210135]
22. Malliaras K, Ibrahim A, Tseliou E, et al. Stimulation of endogenous cardioblasts by exogenous cell therapy after myocardial infarction. EMBO Mol Med 2014:760–77. [PubMed: 24797668]
23. Song L, Wang L, Li F, et al. Bone marrow-derived tenascin-C attenuates cardiac hypertrophy by controlling inflammation. J Am Coll Cardiol 2017;70:1601–15. 24. [PubMed: 28935038]
24. van Amerongen MJ, Harmsen MC, van Rooijen N, Petersen AH, van Luyn MJ. Macrophage depletion impairs wound healing and increases left ventricular remodeling after myocardial injury in mice. Am J Pathol 2007;170:818–29. [PubMed: 17322368]
25. Leblond AL, Klinkert K, Martin K, et al. Systemic and cardiac depletion of M2 macrophage through CSF-1R signaling inhibition alters cardiac function post myocardial infarction. PLoS One 2015;10:e0137515. [PubMed: 26407006]

26. Xia Y, Lee K, Li N, Corbett D, Mendoza L, Frangogiannis NG. Characterization of the inflammatory and fibrotic response in a mouse model of cardiac pressure overload. Histochem Cell Biol 2009;131:471–81. [PubMed: 19030868]
27. Li F, Yang M, Wang L, et al. Autofluorescence contributes to false-positive intracellular Foxp3 staining in macrophages: a lesson learned from flow cytometry. J Immunol Methods 2012;386:101–7. [PubMed: 23046996]
28. Kaikita K, Hayasaki T, Okuma T, Kuziel WA, Ogawa H, takeya M. Targeted deletion of CC chemokine receptor 2 attenuates left ventricular remodeling after experimental myocardial infarction. Am J Pathol 2004;165:439–47. [PubMed: 15277218]
29. Dewald O, Zymek P, Winkelmann K, et al. CCL2/Monocyte Chemoattractant Protein-1 regulates inflammatory responses critical to healing myocardial infarcts. Circ Res 2005;96:881–9. [PubMed: 15774854]
30. Palframan RT, Jung S, Cheng G, et al. Inflammatory chemokine transport and presentation in HEV. a remote control mechanism for monocyte recruitment to lymph nodes in inflamed tissues J Exp Med 2001;194:1361–73. [PubMed: 11696600]
31. Epelman S, Lavine KJ, Beaudin AE, et al. Embryonic and adult-derived resident cardiac macrophages are maintained through distinct mechanisms at steady state and during inflammation. Immunity 2014;40:91–104. [PubMed: 24439267]
32. Leid J, Carrelha J, Boukarabila H, Epelman S, Jacobsen SEW, Lavine KJ. Primitive embryonic macrophages are required for coronary development and maturation. Circ Res 2016;118:1498–511. [PubMed: 27009605]
33. Nahrendorf M, Swirski FK, Aikawa E, et al. The healing myocardium sequentially mobilizes two monocyte subsets with divergent and complementary functions. J Exp Med 2007;204:3037–47. [PubMed: 18025128]
34. Jung K, Kim P, Leuschner F, et al. Endoscopic time-lapse imaging of immune cells in infarcted mouse hearts. Circ Res 2013;112:891–9. [PubMed: 23392842]
35. Hilgendorf I, Gerhardt LMS, Tan TC, et al. Ly-6C^{high} monocytes depend on Nr4a1 to balance both inflammatory and reparative phases in the infarcted myocardium. Circ Res 2014;114:1611–22. [PubMed: 24625784]
36. Hanna RN, Carlin LM, Hubbeling HG, et al. The transcription factor NR4A1 (Nur77) controls bone marrow differentiation and the survival of Ly6C^{-} monocytes. Nat Immunol 2011;12:778–85. [PubMed: 21725321]
37. Leuschner F, Rauch PJ, Ueno T, et al. Rapid monocyte kinetics in acute myocardial infarction are sustained by extramedullary monocytopoiesis. J Exp Med. 2012;209:123–37. [PubMed: 22213805]
38. Heidt T, Courties G, Dutta P, et al. Differential contribution of monocytes to heart macrophages in steady-state and after myocardial infarction. Circ Res 2014;115:284–95. [PubMed: 24786973]
39. Swirski FK, Nahrendorf M, Etzrodt M, et al. Identification of splenic reservoir monocytes and their deployment to inflammatory sites. Science 2009;325:612–6. [PubMed: 19644120]
40. Leuschner F, Panizzi P, Chico-Calero I, et al. Angiotensin-converting enzyme inhibition prevents the release of monocytes from their splenic reservoir in mice with myocardial infarction. Circ Res 2010;107:1364–73. [PubMed: 20930148]
41. Vannella KM, Wynn TA. Mechanisms of organ injury and repair by macrophages. Annu Rev Physiol 2017;79:593–617. [PubMed: 27959618]
42. Auffray C, Fogg D, Garfa M, et al. Monitoring of blood vessels and tissues by a population of monocytes with patrolling behavior. Science 2007;317:666–70. [PubMed: 17673663]
43. Auffray C, Sieweke MH, Geissmann F. Blood monocytes: development, heterogeneity, and relationship with dendritic cells. Annu Rev Immunol 2009;27:669–92. [PubMed: 19132917]
44. Gordon S Alternative activation of macrophages. Nat Rev Immunol 2003;3:23–35. [PubMed: 12511873]
45. Gordon S, Martinez FO. Alternative activation of macrophages: mechanism and functions. Immunity 2010;32:593–604. [PubMed: 20510870]
46. Martinez FO, Gordon S. The M1 and M2 paradigm of macrophage activation: time for reassessment. F1000Prime Rep 2014;6:13. [PubMed: 24669294]

47. Wang C, Yu X, Cao Q, et al. Characterization of murine macrophages from bone marrow, spleen and peritoneum. BMC Immunol 2013;14:6. [PubMed: 23384230]
48. Bisgaard LS, Mogensen CK, Rosendahl A, et al. Bone marrow-derived and peritoneal macrophages have different inflammatory response to oxLDL and M1/M2 marker expression – implications for atherosclerosis research. Sci Rep 2016;6:35234. [PubMed: 27734926]
49. Scheinman EJ, Avni O. Transcriptional regulation of GATA3 in T helper cells by the integrated activities of transcription factors downstream of the interleukin-4 receptor and T cell receptor. J Biol Chem 2009;284:3037–48. [PubMed: 19056736]
50. Barbul A Proline precursors to sustain mammalian collagen synthesis. J Nutr 2008;138:2021S–2024S. [PubMed: 18806118]
51. Albina JE, Abate JA, Mastrofrancesco B. Role of ornithine as a proline precursor in healing wounds. J Surg Res 1993;55:97–102. [PubMed: 8105150]
52. Mills C Macrophage arginine metabolism to ornithine/urea or nitric oxide/citrulline: a life or death issue. Crit Rev Immunol 2001;21:399–425. [PubMed: 11942557]
53. Hesse M, Modolell M, La Flamme AC, et al. Differential regulation of nitric oxide synthase-2 and arginase-1 by type 1/type 2 cytokines in vivo: granulomatous pathology is shaped by the pattern of L-arginine metabolism. J Immunol 2001;167:6533–44. [PubMed: 11714822]
54. Yang Z, Grinchuk V, Urban JF, Jr., et al. Macrophages as IL-25/IL-33-responsive cells play an important role in the induction of type 2 immunity. PLoS One 2013;8:e59441. [PubMed: 23536877]
55. Kim EJ, Kim S, Kang DO, Seo HS. Metabolic activity of the spleen and bone marrow in patients with acute myocardial infarction evaluated by ^{18}F-fluorodeoxyglucose positron emission tomograpic imaging. Circ Cardiovasc Imag 2014;7:454–60.
56. Frangogiannis NG. The inflammatory response in myocardial injury, repair, and remodelling. Nat Rev Cardiol 2014;11:255–65. [PubMed: 24663091]
57. Lin SL, Castaño AP, Nowlin BT, Lupher ML, Duffield JS. Bone marrow Ly6C^{high} monocytes are selectively recruited to injured kidney and differentiate into functionally distinct populations. J Immunol 2009;183:6733–43. [PubMed: 19864592]
58. Perdiguero E, Sousa-Victor P, Ruiz-Bonilla V, et al. p38/MKP-1–regulated AKT coordinates macrophage transitions and resolution of inflammation during tissue repair. J Cell Biol 2011;195:307–22. [PubMed: 21987635]
59. Osterholzer JJ, Olszewski MA, Murdock BJ, et al. Implicating exudate macrophages and Ly-6C^{high} monocytes in CCR2-dependent lung fibrosis following gene-targeted alveolar injury. J Immunol 2013;190:3447–57. [PubMed: 23467934]
60. Zasłona Z, Przybranowski S, Wilke C, et al. Resident alveolar macrophages suppress, whereas recruited monocytes promote, allergic lung inflammation in murine models of asthma. J Immunol 2014;193:4245–53. [PubMed: 25225663]
61. Weisheit C, Zhang Y, Faron A, et al. Ly6C^{low} and not Ly6C^{high} macrophages accumulate first in the heart in a model of murine pressure-overload. PLoS One 2014;9:e112710. [PubMed: 25415601]
62. Satoh T, Nakagawa K, Sugihara F, et al. Identification of an atypical monocyte and committed progenitor involved in fibrosis. Nature 2017;541:96–101. [PubMed: 28002407]
63. Yancy CW, Jessup M, Bozkurt B, et al. 2013 ACCF/AHA guideline for the management of heart failure. a report of the American College of Cardiology Foundation/American Heart Association Task Force on Practice Guidelines J Am Coll Cardiol 2013;62:e147–239. [PubMed: 23747642]
64. Authors/Task Force Members, McMurray JJV, Adamopoulos S, et al. ESC Guidelines for the diagnosis and treatment of acute and chronic heart failure 2012: The Task Force for the Diagnosis and Treatment of Acute and Chronic Heart Failure 2012 of the European Society of Cardiology. Developed in collaboration with the Heart Failure Association (HFA) of the ESC. Eur Heart J 2012;33:1787–847. [PubMed: 22611136]
65. Huaux F, Liu T, McGarry B, Ullenbruch M, Phan SH. Dual roles of IL-4 in lung injury and fibrosis. J Immunol 2003;170:2083–92. [PubMed: 12574379]
66. Borthwick LA, Wynn TA, Fisher AJ. Cytokine mediated tissue fibrosis. Biochim Biophys Acta 2013;1832:1049–60. [PubMed: 23046809]

67. Gao Q, Li Y, Li M. The potential role of IL-33/ST2 signaling in fibrotic diseases. J Leukoc Biol 2015;98:15–22. [PubMed: 25881899]

68. Kurowska-Stolarska M, Stolarski B, Kewin P, et al. IL-33 amplifies the polarization of alternatively activated macrophages that contribute to airway inflammation. J Immunol 2009;183:6469–77. [PubMed: 19841166]

69. Li D, Guabiraba R, Besnard AG, et al. IL-33 promotes ST2-dependent lung fibrosis by the induction of alternatively activated macrophages and innate lymphoid cells in mice. J Allergy Clin Immunol 2014;134:1422–1432.e11. [PubMed: 24985397]

70. Carlson S, Helterline D, Asbe L, et al. Cardiac macrophages adopt profibrotic/M2 phenotype in infarcted hearts: role of urokinase plasminogen activator. J Mol Cell Cardiol 2017;108:42–9. [PubMed: 27262672]

71. Vannella KM, Barron L, Borthwick LA, et al. Incomplete deletion of IL-4Rα by $LysM^{Cre}$ reveals distinct subsets of M2 macrophages controlling inflammation and fibrosis in chronic schistosomiasis. PLoS Pathogens 2014;10:e1004372. [PubMed: 25211233]

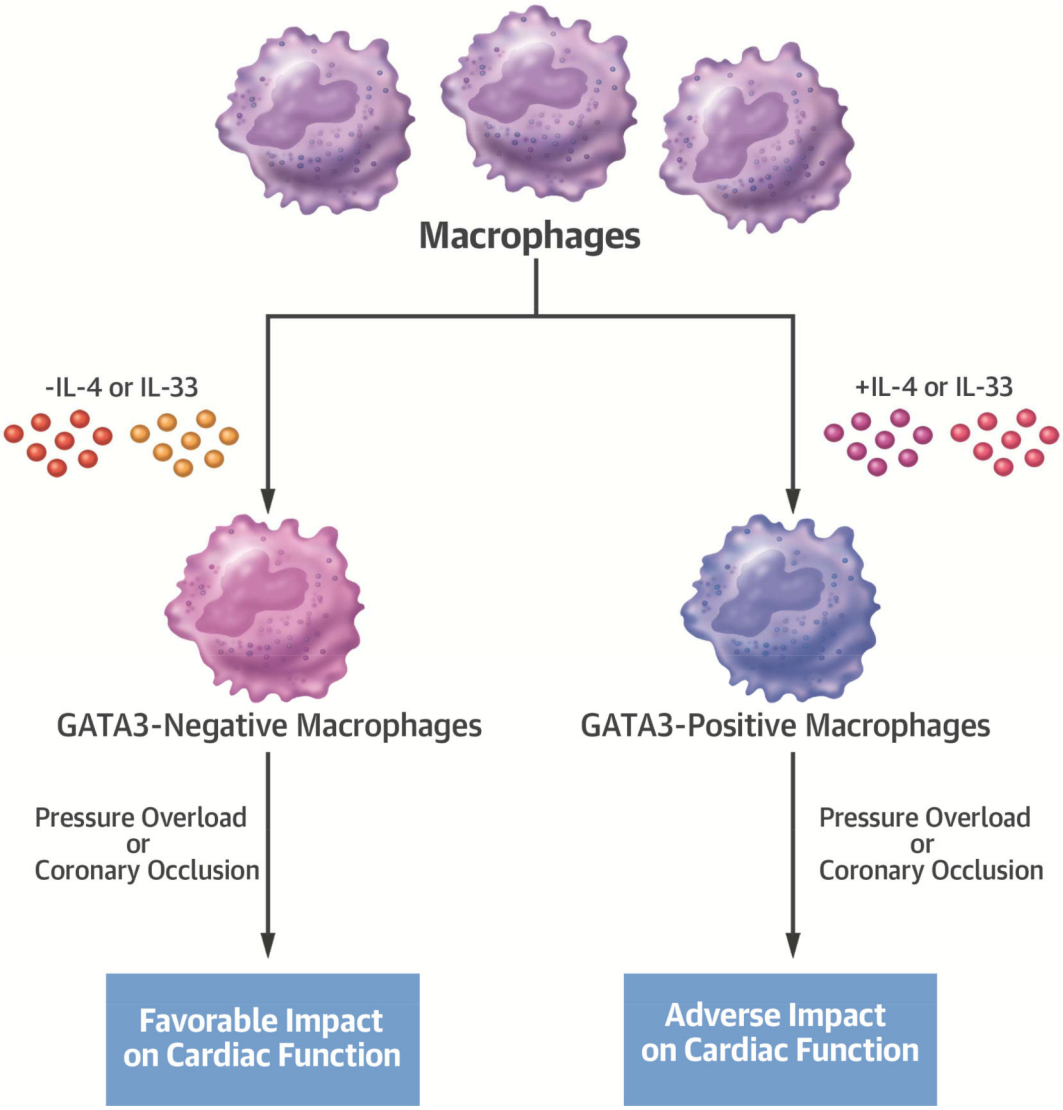

Central Illustration: Macrophage GATA3 Expression Modulates Cardiac Function after Pressure Overload or Coronary Occlusion.

A comparison of the effect of macrophage subsets (GATA3-positive vs. GATA3-negative) on cardiac disease. GATA3 expression in macrophages is induced by the IL-4 or IL-33 cytokines. The presence of the GATA3-positive subset adversely affects cardiac function in response to coronary osculation or pressure overload. Conversely, the absence of this macrophage subset has a favorable impact on cardiac function. IL = interleukin.

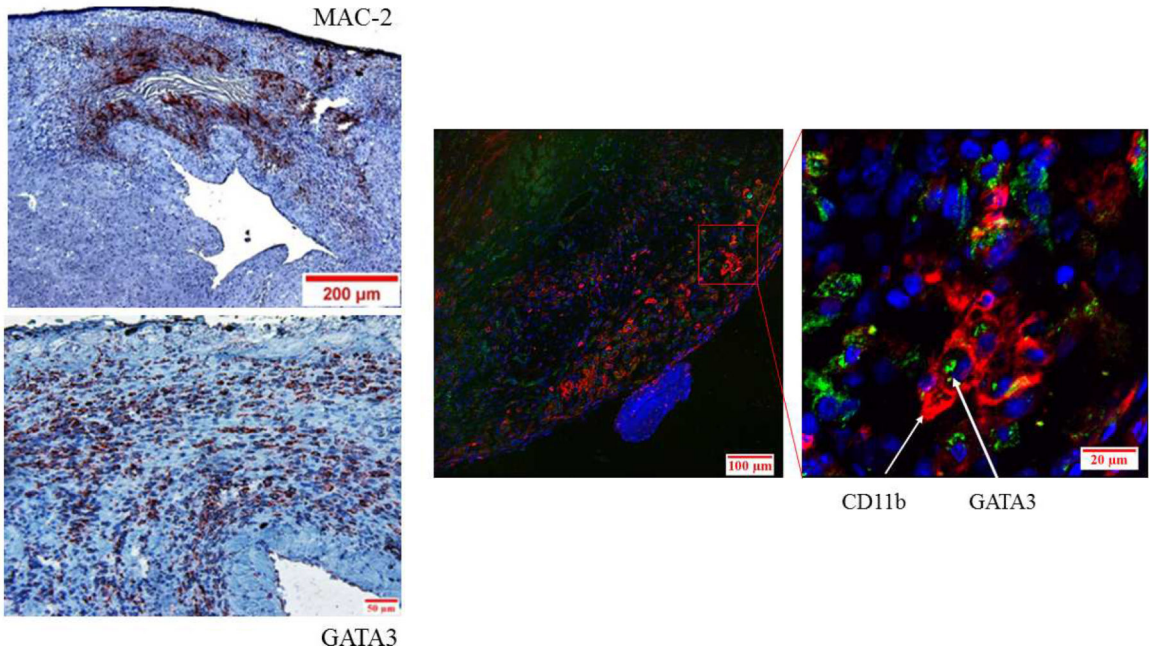

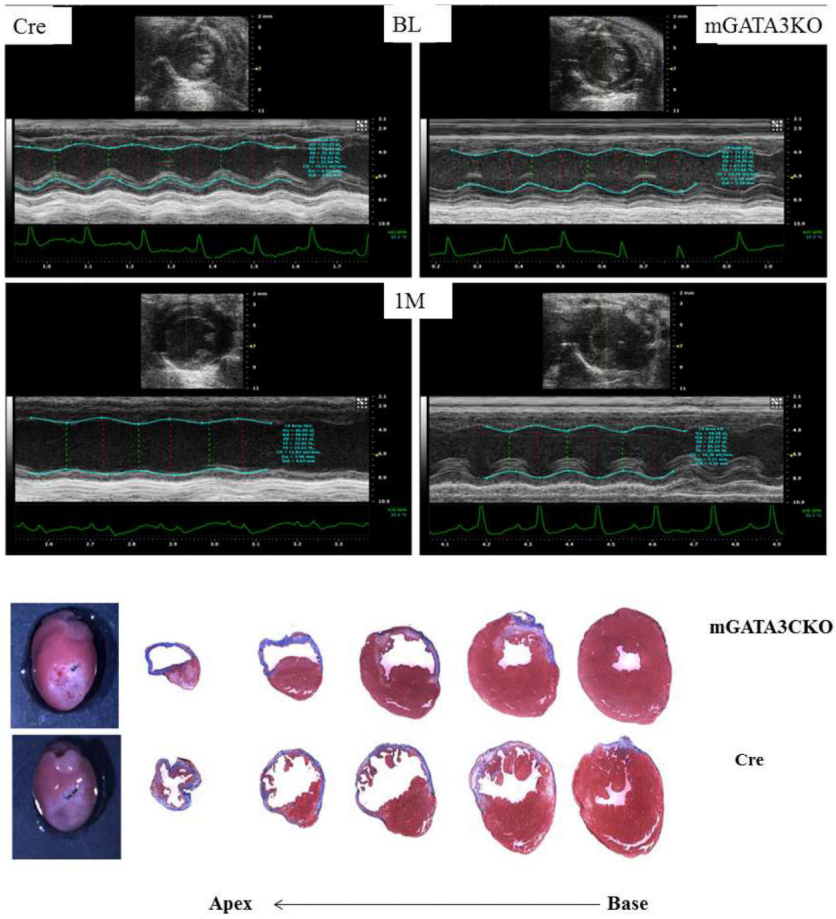

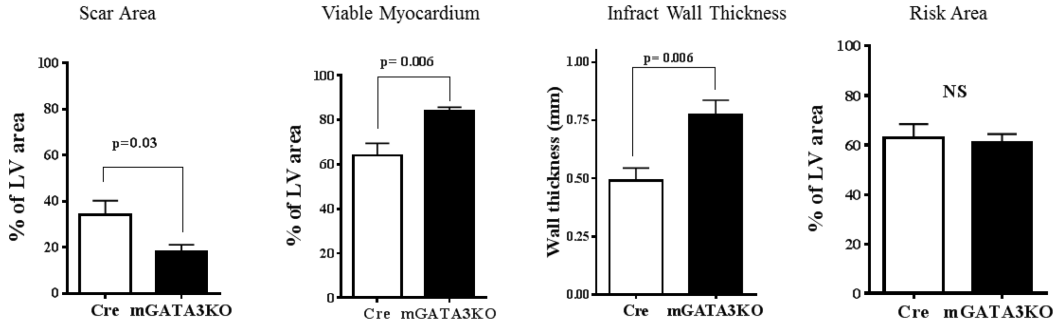

Figure 1. Deficiency of GATA3-Positive Macrophages Improved Cardiac Function After MI.

(A) Representative immunostaining of LV sections from control Cre mice. Serial sections of LVs from control Cre mice at 8 days post-MI were stained with anti–Mac-2 or anti-GATA3 antibodies. GATA3-positive staining is clearly visible in the infarcted region of the myocardium, which contains large numbers of macrophages, but not in the healthy region. Sections were also stained with fluorescent-labeled antibodies to demonstrate the nuclear colocalization of GATA3 in macrophages located in the infarcted region of the myocardium. (**B**) Representative M-mode echocardiograms from the 2 groups of mice before (BL) and 1 month after MI (1M). (**C**) Representative photographs of Masson Trichrome staining from sections from the base to the apex of hearts from the 2 mice genotype groups. Photographs of all of the hearts are shown in **Online Figure 3**. (**D**) Morphometric analysis of each heart section. The number of animals in each group is shown in **Table 1**. LV = left ventricle; mGATA3KO = myeloid-specific GATA3 knockout mouse; MI = myocardial infarction.

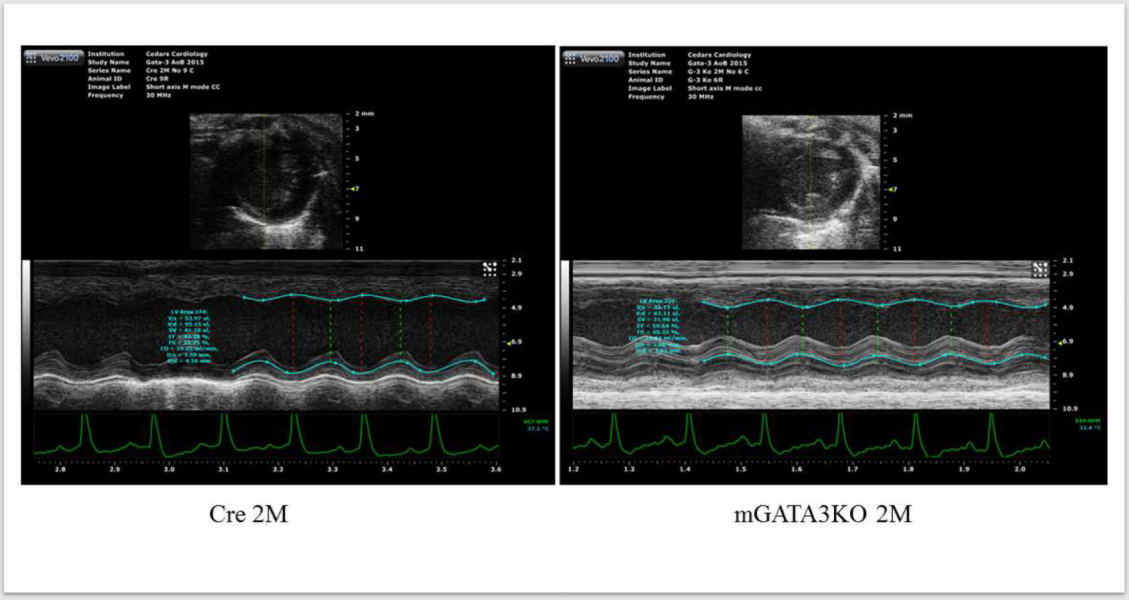

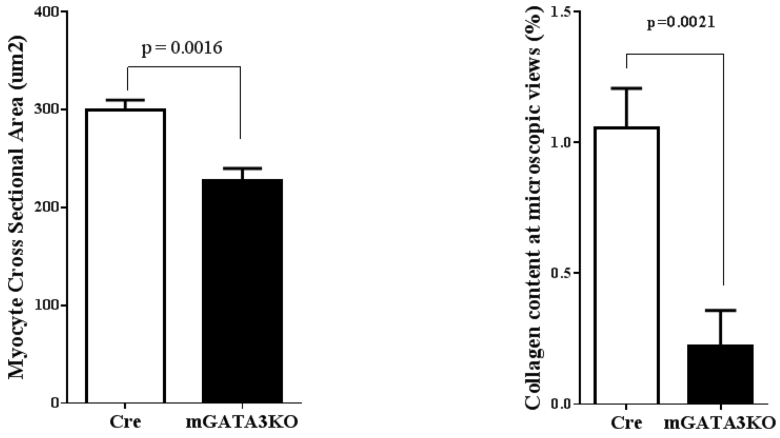

Figure 2. Macrophage-Specific GATA3 Deficiency Protects Myocardium Against Pressure Overload-Induced Hypertrophy.

(**A**) Representative M-mode echocardiographic data from the 2 mouse genotypes at 2 months after transverse aortic constriction. (**B**) Harvested hearts were analyzed to determine the size of cardiomyocytes and collagen content. N = 5 mice/genotype. The number of animals in each group is shown in **Table 2**. mGATA3KO = myeloid-specific GATA3 knockout mouse.

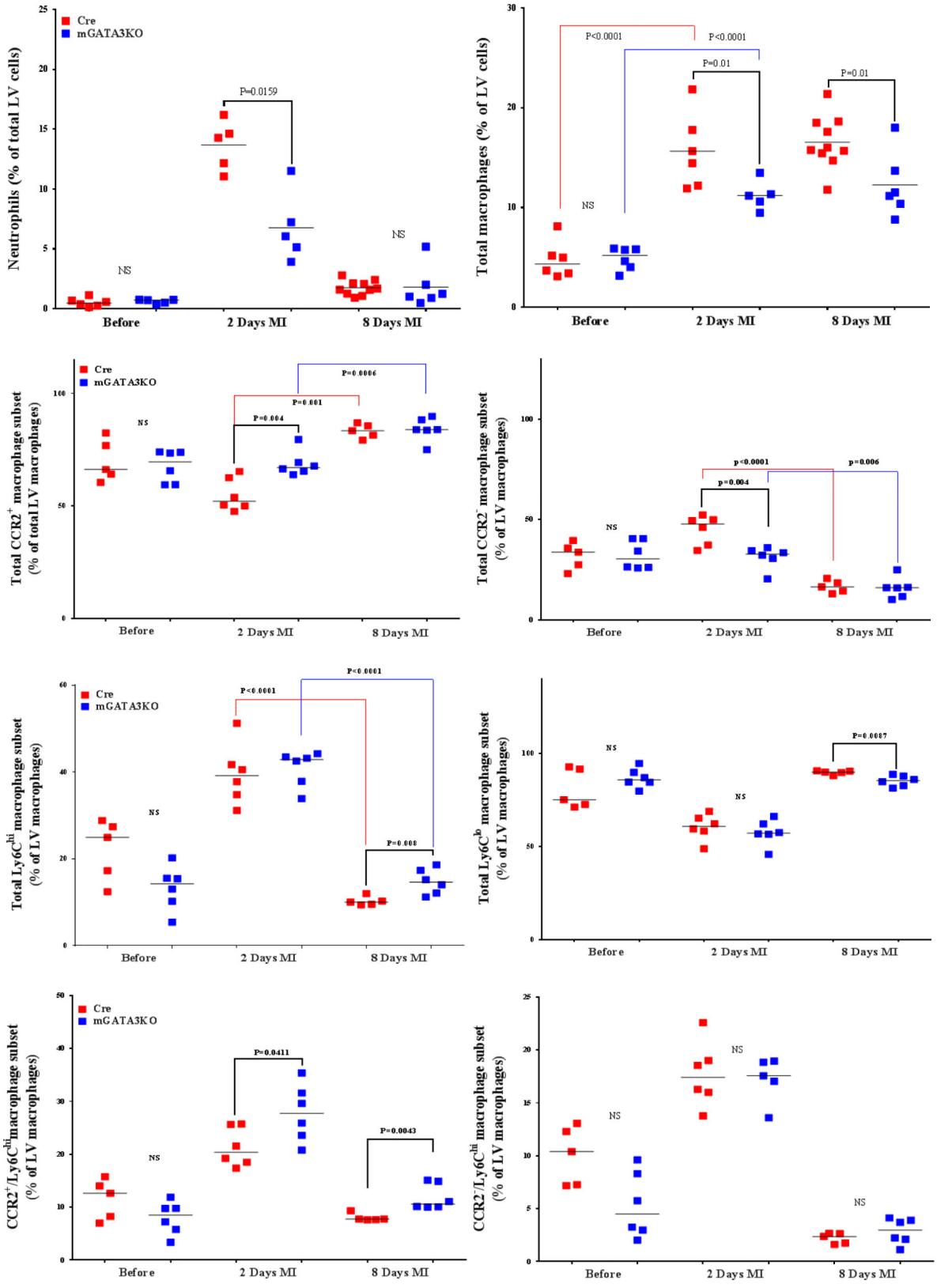

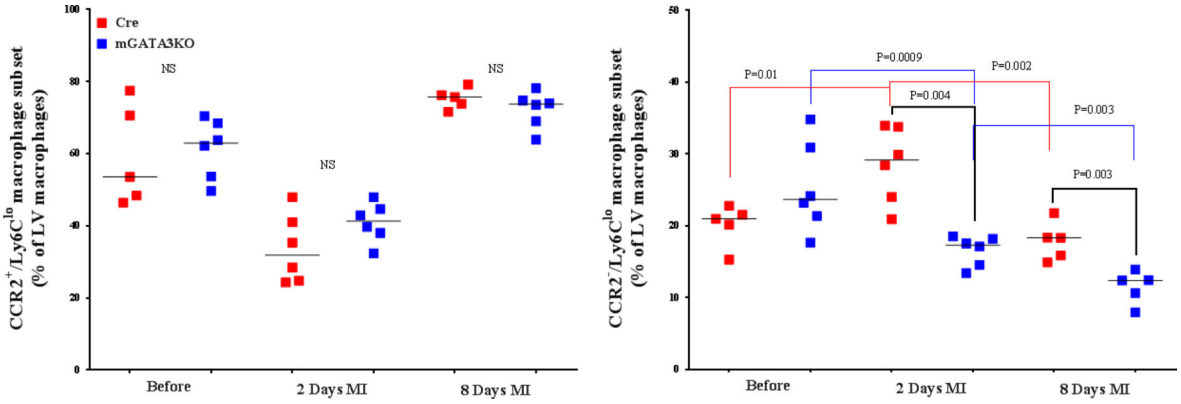

Figure 3. Phenotype of Monocytes/Macrophages in the LV of the 2 Mouse Genotypes.

LVs from the 2 mouse genotypes before and at the indicated days after MI were digested, stained with appropriate antibodies, and analyzed by flow cytometry to determine monocyte and macrophage phenotypes. Each panel depicts a specific cell subset based on the expression of cell markers. **(A)** neutrophils (left) and total macrophages (right); **(B)** total $CCR2^{+}$ (left) and $CCR2^{-}$ macrophage subsets (right); **(C)** total $Ly6C^{hi}$ (left) and total $Ly6C^{lo}$ macrophage subsets (right); **(D)** $CCR2^{+}/Ly6C^{hi}$ (left) and $CCR2^{-}/Ly6C^{hi}$ macrophage subsets (right); **(E)** $CCR2^{+}/Ly6C^{lo}$ (left) and $CCR2^{-}/Ly6C^{lo}$ macrophage subsets (right). Each data point represents 1 mouse/genotype. Total $CCR2^{+}$, $CCR2^{-}$, $Ly6C^{hi}$, or $Ly6C^{lo}$ cells were calculated by addition of the frequencies of each cell subset. Data from the 2 groups (Cre versus mGATA3KO) before and after MI were analyzed by Student *t*-test. Each data point represents 1 mouse; therefore, the number of animals in each group is equal to the number of dots/group. Abbreviations as in **Figure 1**.

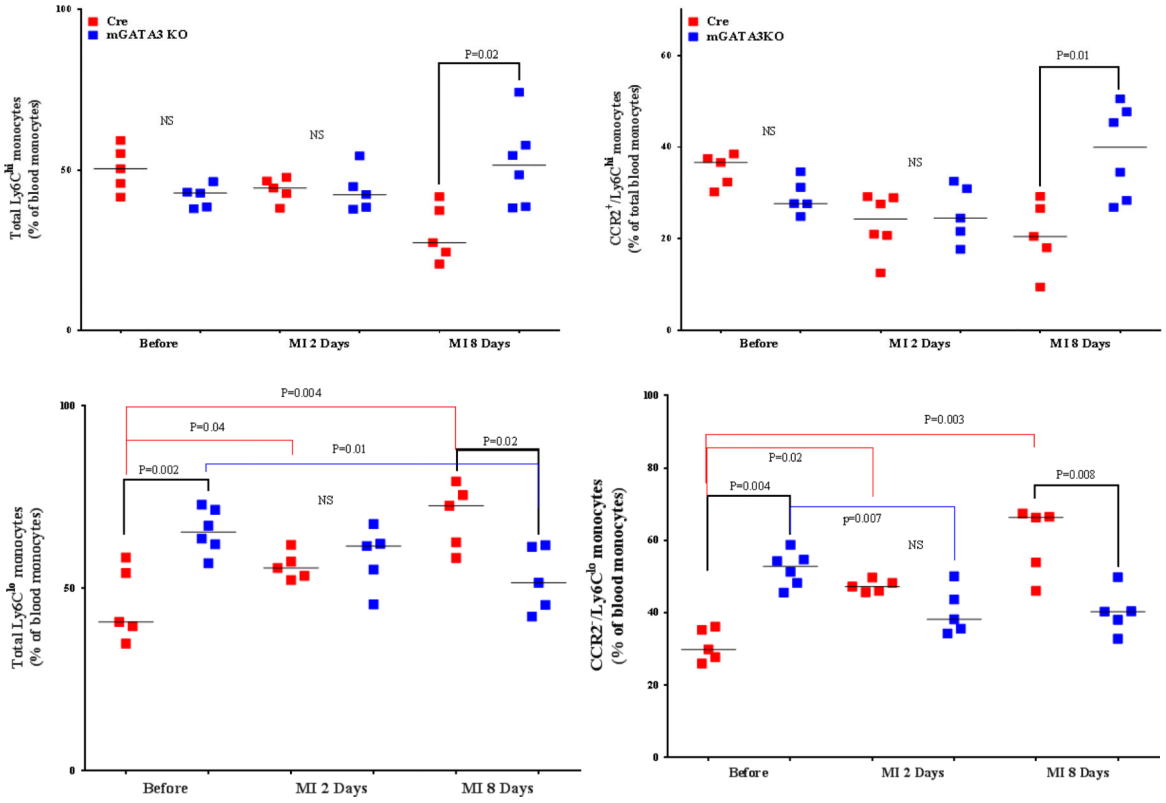

Figure 4. Phenotype of Monocytes in Peripheral Blood From the 2 Mouse Genotypes.

Peripheral blood was collected from the 2 mouse genotype groups before and at the indicated days after MI, stained with the appropriate antibodies, and analyzed by flow cytometry, essentially as described in **Figure 3** using the gating strategy outlined in **Online Figure 4**. Each panel depicts a specific cell subset based on the expression of cell markers; **(A)** Left: $CCR2^{+}/Ly6C^{hi}$ monocytes; right: $CCR2^{-}/Ly6C^{hi}$ monocytes. **(B)** Left: total $Ly6C^{lo}$ monocytes; right: $CCR2^{-}/Ly6C^{lo}$ monocyte subset. Each data point represents a blood sample from an individual mouse. The number of animals in each group is equal to the number of dots/group. MI = myocardial infarction; NS = not significant.

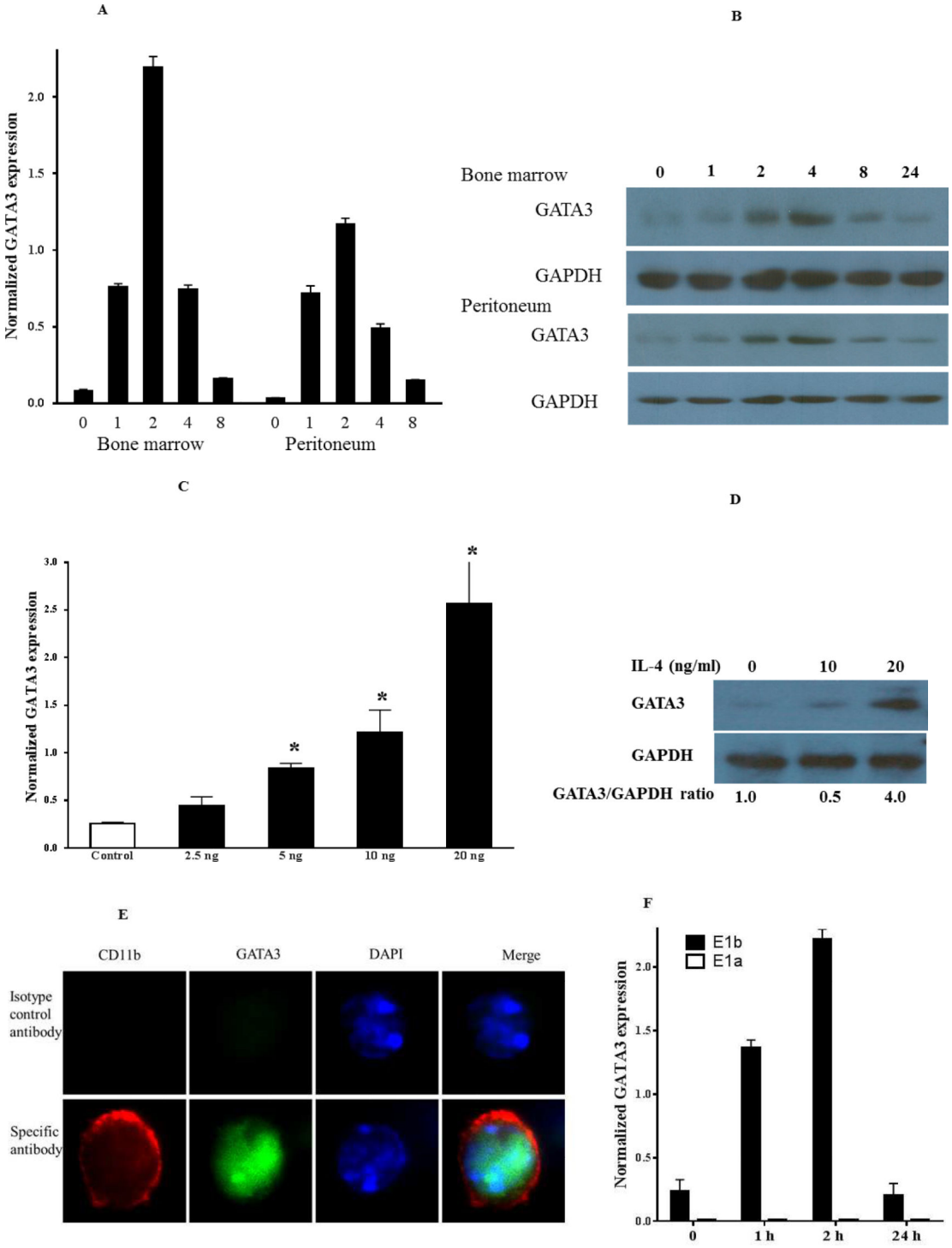

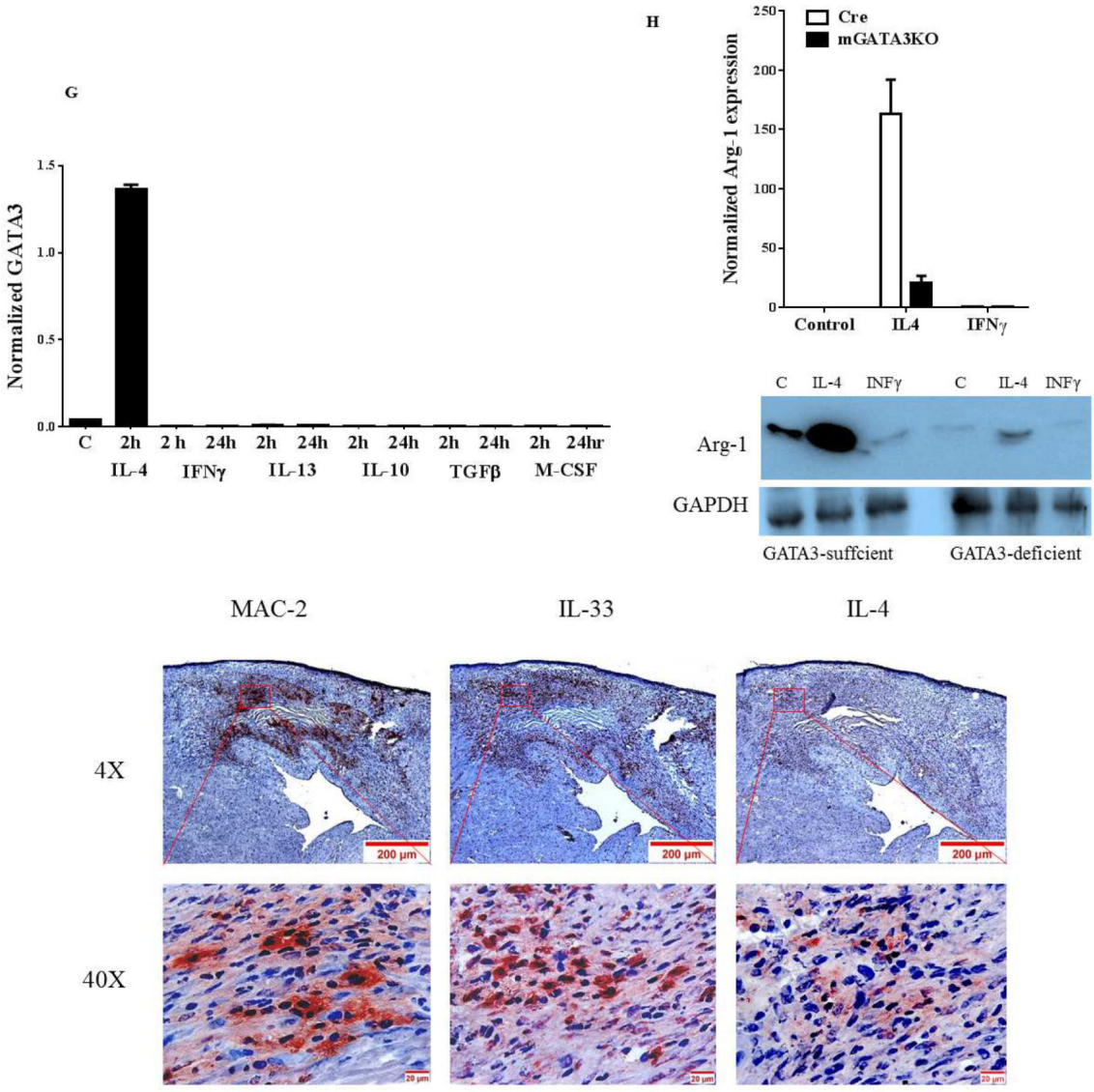

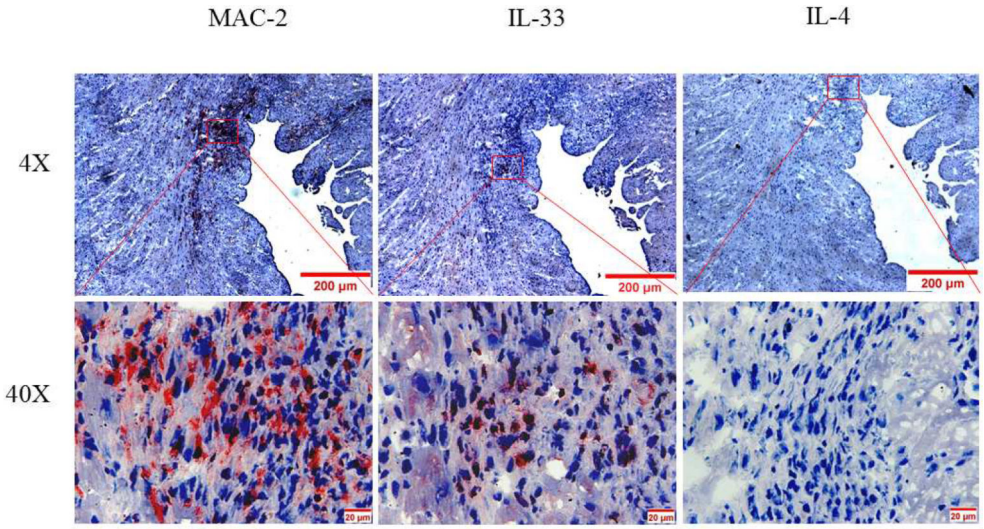

Figure 5. Mechanism of GATA3 Expression in Macrophages.

(A) Macrophages were isolated from the peritoneum or the bone marrow of control Cre mice and cultured. Cultured cells were treated with IL-4 at the indicated times, and GATA3 expression was evaluated by qPCR. GATA3 gene expression data were normalized against GAPDH. Results are the mean of triplicate determinations ± SD. (**B**) Proteins were extracted from cells treated with 20 ng/ml of IL-4 at the indicated times. (**C**) Dose-response analysis of GATA3 expression was determined by qPCR using cultured macrophages isolated from the bone marrow of control mice. (**D**) Proteins were analyzed by western blot analysis of lysates from cells treated with 10 or 20 ng/ml of IL-4. (**E**) Bone marrow-derived macrophages were plated onto chamber slides and treated with 20 ng/ml IL-4 for 4 h, followed by staining with the indicated fluorescent antibodies. Isotypematched antibodies were used as controls. (**F**) Total RNA was isolated from cultured bone marrow-derived macrophages from Cre mice treated with IL-4 at the indicated times and analyzed by qPCR using primers specific to the proximal (E1b) or distal (E1a) GATA3 promoter. GATA3 gene expression data were normalized against the GAPDH gene. (**G**) Cultured bone marrow-derived macrophages were treated with the indicated agonists for 2 and 24 h. Total RNA was extracted and analyzed by qPCR, and the resulting GATA3 data were normalized against GAPDH. (**H**) Cultured bone marrow-derived macrophages from the indicated mouse genotype were treated with IL-4 or IFNγ for 2 h, followed by isolation of total RNA. qPCR data for Arg-1 expression were normalized against GAPDH gene expression. In addition, proteins were extracted from the treated cells and analyzed by western blot using an antibody to Arg-1. All qPCR results are means of triplicate determinations ± SD. *Indicates a significant difference between control and treated cells, $p < 0.05$. (**I**) Representative immunostaining data for IL-4 or IL-33 expression in LV sections from control mice at 8 days post-MI. (**J**) Representative immunostaining of the LV section from the mGATA3KO mice stained with antibodies to Mac-2, IL-4, or IL-33. The upper panels show low magnification and the lower panels show high magnification. Arg-1 = arginase-1; GAPDH = glyceraldehyde 3-phosphate dehydrogenase IFN = interferon; IL = interleukin; qPCR = quantitative real-time polymerase chain reaction. Other abbreviations as in **Figure 1**.

Table 1.

Pooled Echocardiographic Data From the 2 Mouse Genotypes Under Basal Conditions (Before MI) and 1 Month Post-MI

	Baseline			Post-MI		
	Cre	**mGATA3KO**	**p Value**	**Cre**	**mGATA3KO**	**p Value**
Number of animals	5	6		6	6	
Heart rate	405 ± 19	423 ± 14	NS	443 ± 27	425 ± 17	NS
EF (%)	63.3 ± 0.2	63.4 ± 0.8	NS	44.2 ± 1.9	53.81+1.1	<0.001
FS (%)	33.7 ± 0.1	33.7 ± 0.6	NS	21.8 ± 1.1	27.4 ± 0.7	0.002
EDV (μl)	58.7 ± 2.1	56.4 ± 1.8	NS	82.5 ± 6.3	67.27 ± 2.2	0.04
ESV (μl)	21.9 ± 0.7	20.7 ± 0.9	NS	82.5 ± 6.3	67.2 ± 2.2	0.04

Values are mean percent changes over baseline.

EDV = end-diastolic volume; EF = ejection fraction; ESV = end-systolic volume; FS = fractional shortening; mGATA3KO = myeloid-specific GATA3 knockout mouse; MI = myocardial infarction; NS = not significant.

Table 2.

Echocardiographic Assessment and Heart Mass Ratios of the 2 Mouse Genotypes 2 Months Post-TAC

	Cre	mGATA3KO	p Value
Number of animals	8	6	
Heart rate	426 ± 36	435 ± 18	NS
EF (%)	41.3 ± 0.9	50.6 ± 0.4	<0.0001
FS (%)	20.9 ± 0.6	25.3 ± 0.2	0.0002
ESV	52.5 ± 2.0	33.5 ± 1.1	<0.0001
EDV	92.8 ± 3.3	67.2 ± 1.8	<0.0001
LVPWTs	1.05 ± 0.01	0.93 ± 0.02	<0.001
LVPWTd	0.84 ± 0.01	0.70 ± 0.02	<0.0005
HW/BW	5.8 ± 0.3	4.5 ± 0.1	<0.02

Values are mean ± SD. HW/BW at baseline for Cre and mGATA3KO mice were 4.1 ± 0.14 and 3.99 ± 0.15, respectively.

HW/BW = heart weight per body weight ratio; LVPWTd = LV posterior wall thickness diastolic; LVPWTs = left ventricular posterior wall thickness systolic; TAC = transverse aortic constriction. Other abbreviations as in **Table 1**.